

This is a repository copy of *Unveiling the mechanism of hydrotrophy : evidence for water-mediated aggregations of hydrotrope around the solute*.

White Rose Research Online URL for this paper:

<https://eprints.whiterose.ac.uk/161074/>

Version: Accepted Version

Article:

Abranches, Dinis O, Benfica, Jordana, Soares, Bruna P. et al. (6 more authors) (2020) Unveiling the mechanism of hydrotrophy : evidence for water-mediated aggregations of hydrotrope around the solute. *Chemical Communications*. pp. 7143-7146. ISSN 1364-548X

<https://doi.org/10.1039/d0cc03217d>

Reuse

Items deposited in White Rose Research Online are protected by copyright, with all rights reserved unless indicated otherwise. They may be downloaded and/or printed for private study, or other acts as permitted by national copyright laws. The publisher or other rights holders may allow further reproduction and re-use of the full text version. This is indicated by the licence information on the White Rose Research Online record for the item.

Takedown

If you consider content in White Rose Research Online to be in breach of UK law, please notify us by emailing eprints@whiterose.ac.uk including the URL of the record and the reason for the withdrawal request.

Electronical Supplementary Information

Unveiling the Mechanism of Hydrotropy: Evidence for Water-Mediated Aggregation of Hydrotropes Around the Solute

Dinis O. Abranches,^a Jordana Benfica,^a Bruna P. Soares,^a Alejandro Leal-Duaso,^b Tânia E. Sintra,^a Elísabet Pires,^b Simão P. Pinho,^c Seishi Shimizu^d and João A. P. Coutinho^{*a}

^a CICECO – Aveiro Institute of Materials, Department of Chemistry, University of Aveiro, 3810-193 Aveiro, Portugal

^b Instituto de Síntesis Química y Catálisis Homogénea (ISQCH-CSIC) Facultad de Ciencias, C.S.I.C. - Universidad de Zaragoza, E-50009 Zaragoza, Spain

^c Centro de Investigação de Montanha (CIMO), Instituto Politécnico de Bragança. Campus de Santa Apolónia, 5300-253 Bragança, Portugal

^d York Structural Biology Laboratory, Department of Chemistry, University of York, Heslington, York YO10 5DD, United Kingdom

*Corresponding author email: jcoutinho@ua.pt

Index

Experimental Details _____ S1

Chemicals

Table S1

¹H-NMR

Table S2

σ -Profile

Table S3

Figures _____ S4

Figures S1-S5

References _____ S11

Experimental Details

Chemicals

The substances experimentally used in this work are reported below in Table S1, along with their CAS number, supplier and purity, and their name abbreviation used throughout this work. The water used was doubly distilled, passed through a reverse osmosis system and later treated with Milli-Q (Millipore, model A10, Billerica, MA, USA). The glycerol ethers used were part of a batch synthesized in a previous work.¹

Table S1. Name, CAS Number, supplier, purity and name abbreviation of the substances used in this work.

Substance	CAS Number	Supplier	Purity (wt%)	Abbreviation
3-Methoxypropane-1,2-diol	623-39-2	Synthesized ^[a]	>98%	[1.0.0]
3-Ethoxypropane-1,2-diol	1874-62-0	Synthesized ^[a]	>99%	[2.0.0]
3-Propoxypropane-1,2-diol	61940-71-4	Synthesized ^[a]	>99%	[3.0.0]
3-Butoxypropane-1,2-diol	624-52-2	Synthesized ^[a]	>99%	[4.0.0]
3-Pentoxypropane-1,2-diol	22636-32-4	Synthesized ^[a]	>99%	[5.0.0]
Gallic Acid	149-91-7	Merck	>99.5%	GA
Syringic Acid	530-57-4	Acros Organics	>98.0%	SA
Deuterium Oxide	7789-20-0	Aldrich	99.9% ^[b]	D ₂ O
3-(trimethylsilyl)propionic-2,2,3,3-d ₄ acid sodium salt	24493-21-8	Eurisotop	99% ^[b]	TMSP-D ₄

[a] Compound belongs to a batch synthesized in a previous work¹. [b] atom %.

¹H-NMR

¹H-NMR spectra were acquired, at 298 K, using a Bruker Avance 300 spectrometer operating at 300.13 MHz (with chemical shifts, $\Delta\delta$, in ppm). All systems were prepared with a hydrotrope molar concentration of 0.4 M in a 1:1 ratio of water and deuterium oxide (using TMSP-D₄ as the internal reference). Five systems were prepared for each hydrotrope, varying the solute and its concentration, as described in Table S2. The aqueous solutions were prepared by adding the solute to the hydrotropic solution. All systems remained in constant agitation (1050 rpm) for 72 h using Thermomixer Eppendorf Comfort equipment, in order to ensure complete homogenization. All samples were filtered using syringe filters (0.45 μ m) to remove possible suspended solid particles.

Table S2. Solute concentration in the hydrotropic systems (0.4 M of hydrotrope) whose $^1\text{H-NMR}$ spectra was measured in this work.

Hydrotrope	Gallic Acid Concentration / mol·kg ⁻¹	Syringic Acid Concentration / mol·kg ⁻¹
[1.0.0]	0	0
	0.06	0.005
	0.12	0.010
[2.0.0]	0	0
	0.06	0.005
	0.12	0.010
[3.0.0]	0	0
	0.06	0.005
	0.12	0.010
[4.0.0]	0	0
	0.06	0.008
	0.12	0.013
[5.0.0]	0	0
	0.06	0.010
	0.12	0.018

σ -Profile

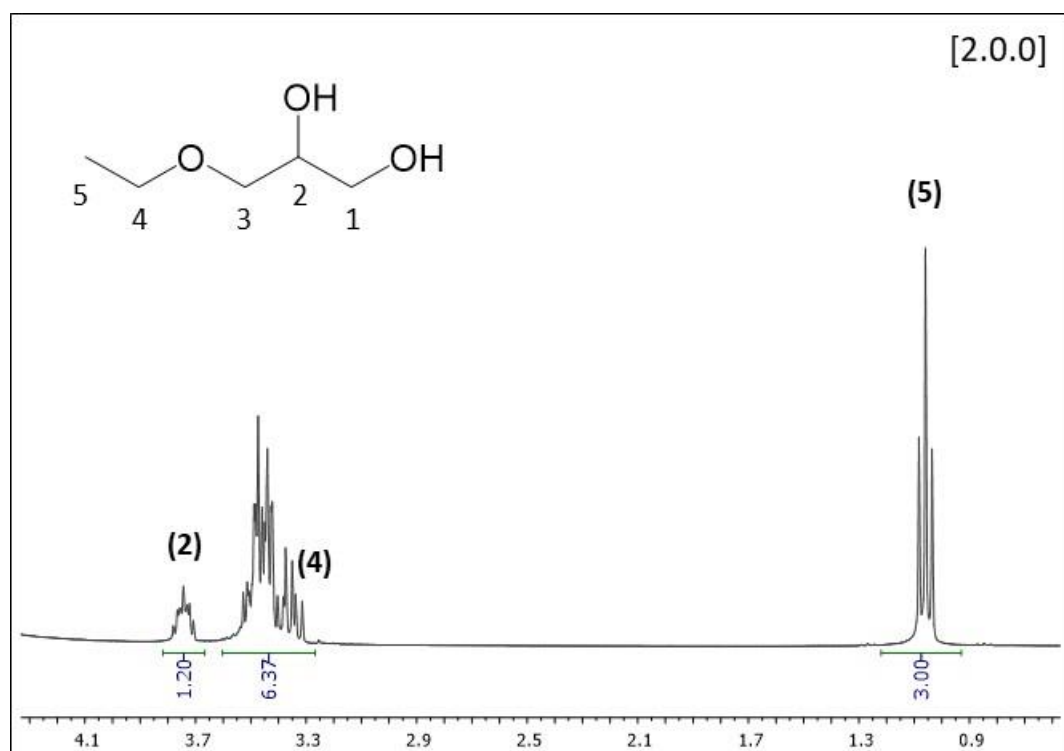
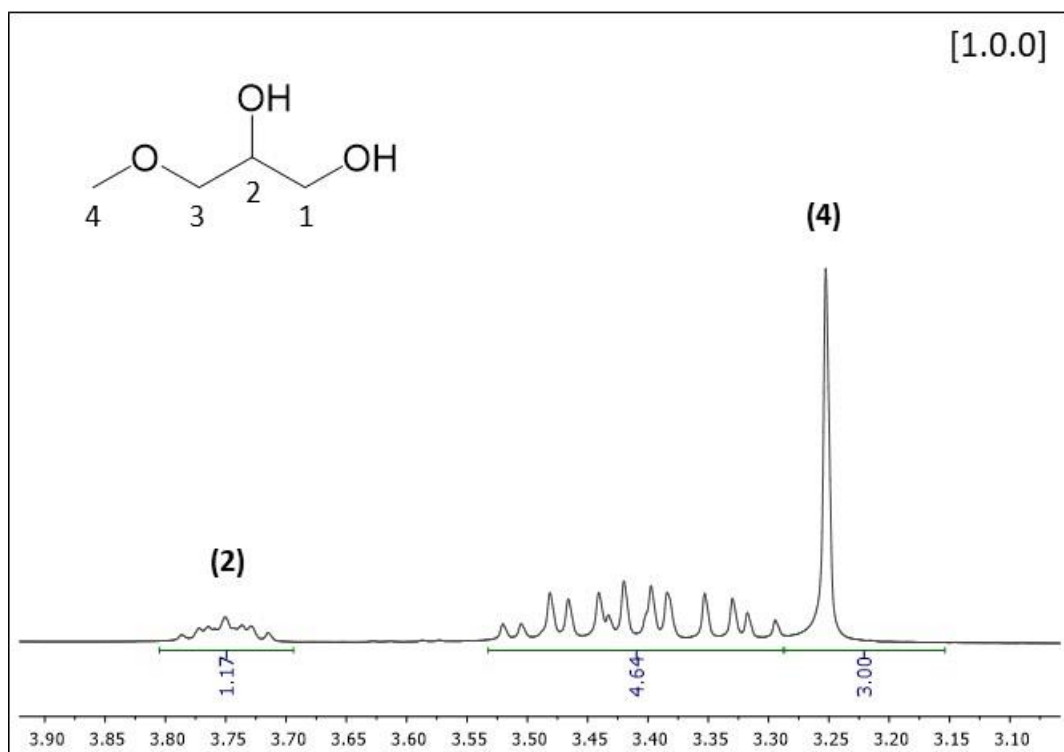
Each molecule (either solute or hydrotrope) was optimized using TURBOMOLE, through its interface TmoleX, by adopting the TZVP template available in the software package.² This template uses a def-TZVP basis set for all atoms, a DFT with the B-P86 functional and the COSMO solvation model (continuum with infinite permittivity). From the molecule file so obtained, the σ -profile of the molecule was computed using the COSMOtherm software with the BP_TZVP_C30_1701 parametrization.^{3,4} For chloride-based ionic liquids, the cation was optimized separately from the chloride anion. The apolar factor of the ionic liquid is obtained by summing the apolar factors of the cation and of the anion.

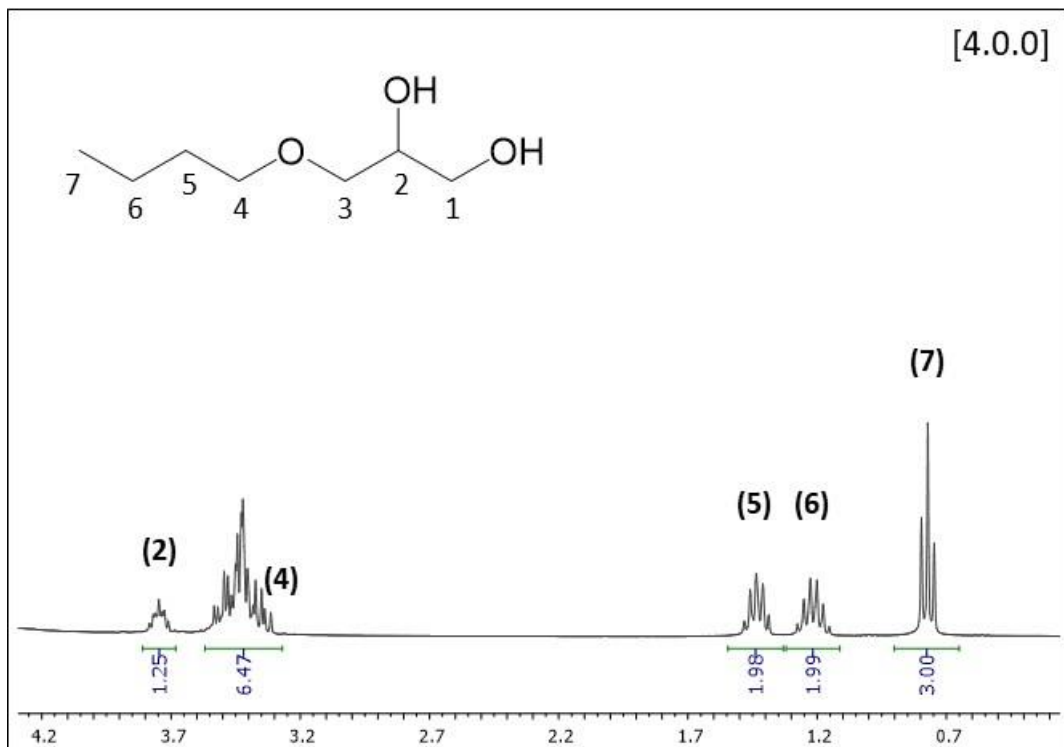
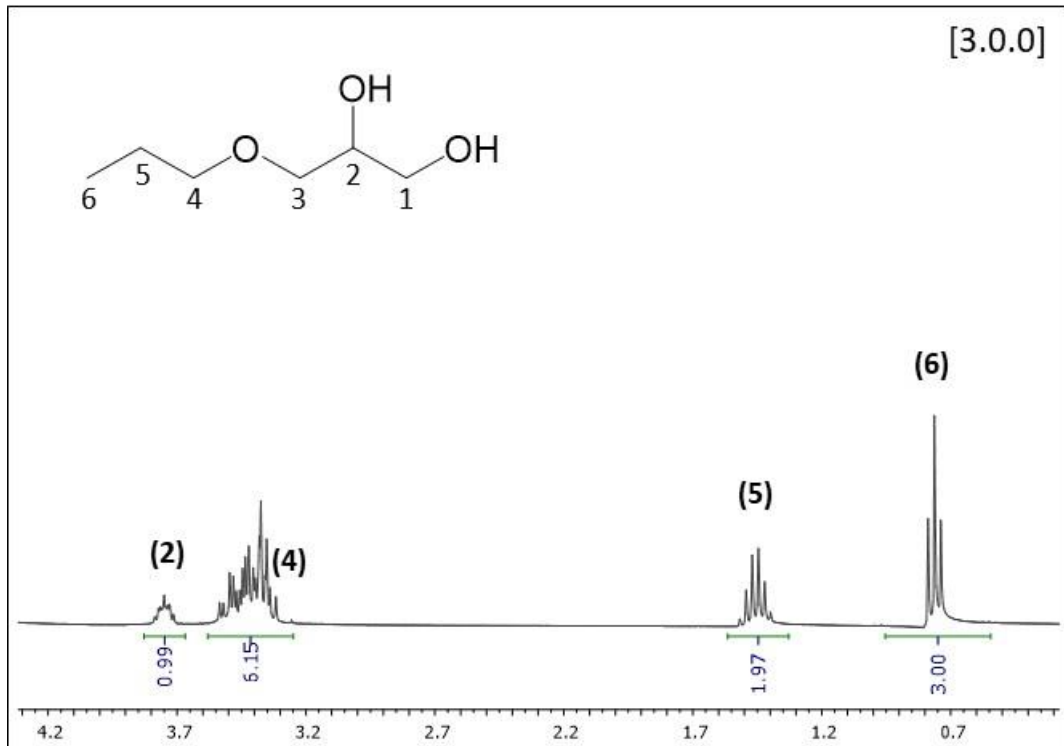
Note that, unlike for the glycerol ether hydrotrope series, the hydrotrope extent of some chloride-based ionic liquids does not correlate well with the corresponding apolar factor (Figure S4). This is most likely due to the role of the chloride ion, which may stay solvated or accumulate around the solute-cation cluster for charge stabilization.

Table S3. *Apolar Factor of substances and ions used in the literature as hydrotropes.*

Substance/Ion	Apolar Factor ($\cdot 10^3$)	Substance/Ion	Apolar Factor ($\cdot 10^3$)
1-ethyl-3-methylimidazolium	0.4755	Chloride	0
1-butyl-3-methylimidazolium	0.7120	Gallic Acid	0.4981
1-hexyl-3-methylimidazolium	0.9684	Syringic Acid	0.7235
1-octyl-3-methylimidazolium	1.2264	[0.0.0]	0.3352
1-butyl-3-methylpyridinium	0.8495	[1.0.0]	0.5041
1-butyl-1-methylpiperidinium	0.7764	[2.0.0]	0.6481
1-butyl-1-methylpyrrolidinium	0.6958	[3.0.0]	0.7820
Tetrabutylammonium	1.6684	[4.0.0]	0.9117
Tetrabutylphosphonium	1.7036	[5.0.0]	1.0406
Cholinium	0.2170	[1.0.1]	0.6828
Sodium	0	[2.0.2]	0.9636

Figures





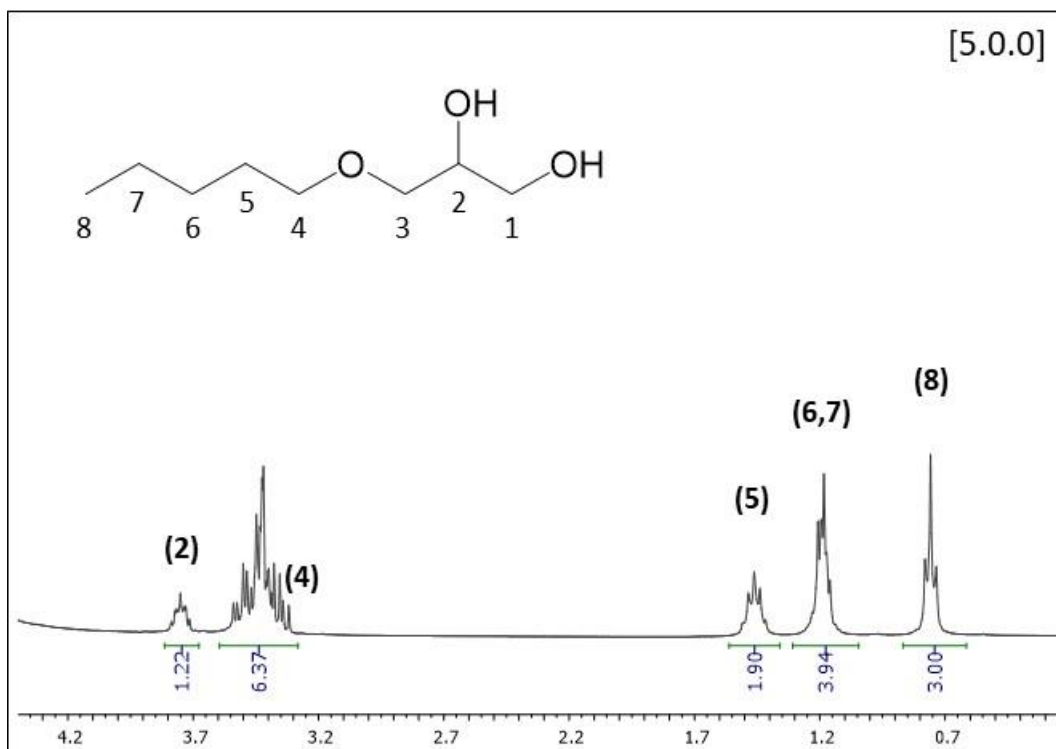


Figure S1. ¹H-NMR spectra for aqueous solutions of monoalkylglycerol ethers (0.4 mol/kg concentration) in the chemical shift window used in this work. From top to bottom, [1.0.0], [2.0.0], [3.0.0], [4.0.0] and [5.0.0], with the structure of each substance reported as inset. Signaled peaks are those used in this work, with the number matching the number sequence of the inset structure. Chemical shifts (x-axis) are reported in ppm.

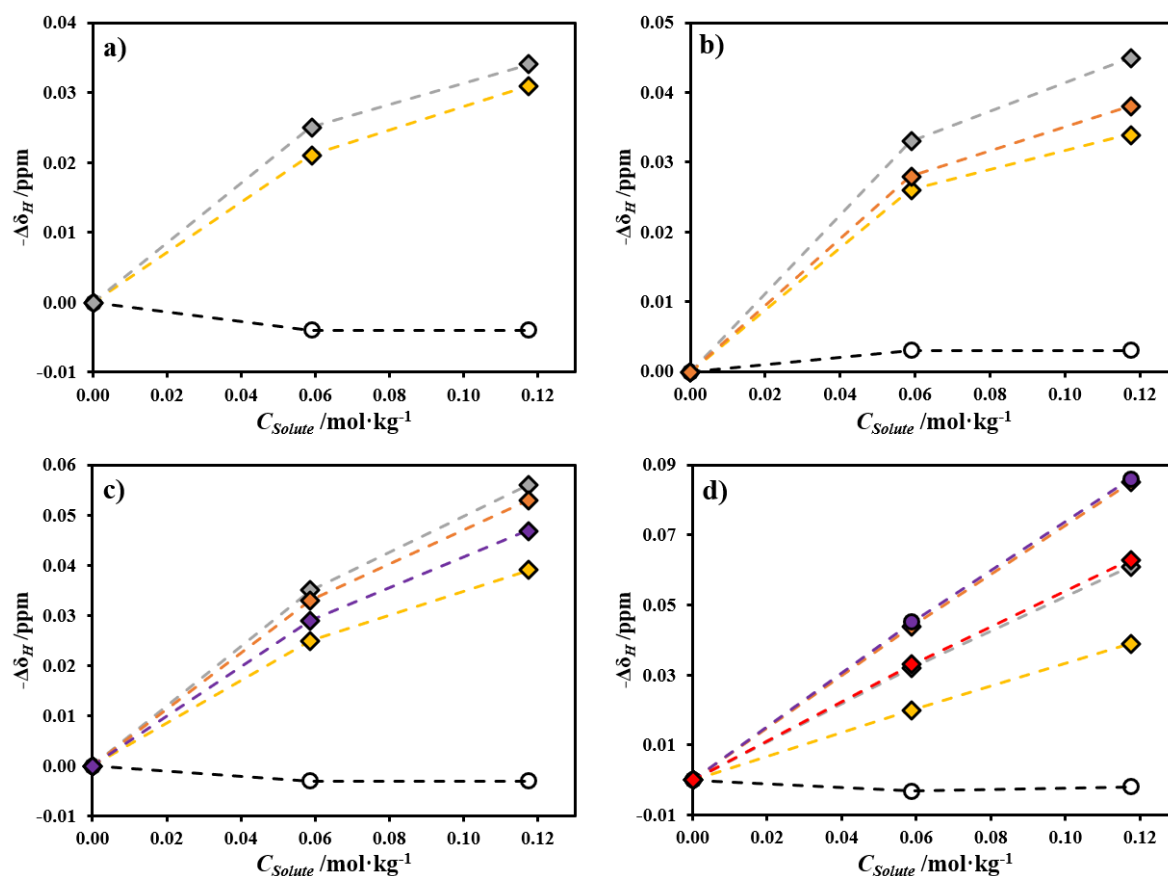


Figure S2. Change in chemical shift of the protons ($-\Delta\delta_H$) associated to water and several methyl groups of a) [1.0.0], b) [2.0.0], c) [3.0.0] and d) [5.0.0] dissolved in water (0.4 mol/kg) as a function of gallic acid concentration. Similar data for [4.0.0] is reported in the main text (Figure 1). Legend: $-\circ-$ water; $-\diamond-$ 2nd carbon; $-\blacklozenge-$ 4th carbon; $-\blacklozenge-$ 5th carbon; $-\blacklozenge-$ 6th carbon; $-\blacklozenge-$ 7th carbon; $-\blacklozenge-$ 8th carbon. For [5.0.0] the peaks from the hydrogens of the 6th and 7th carbon are undistinguishable and are represented as $-\bullet-$.

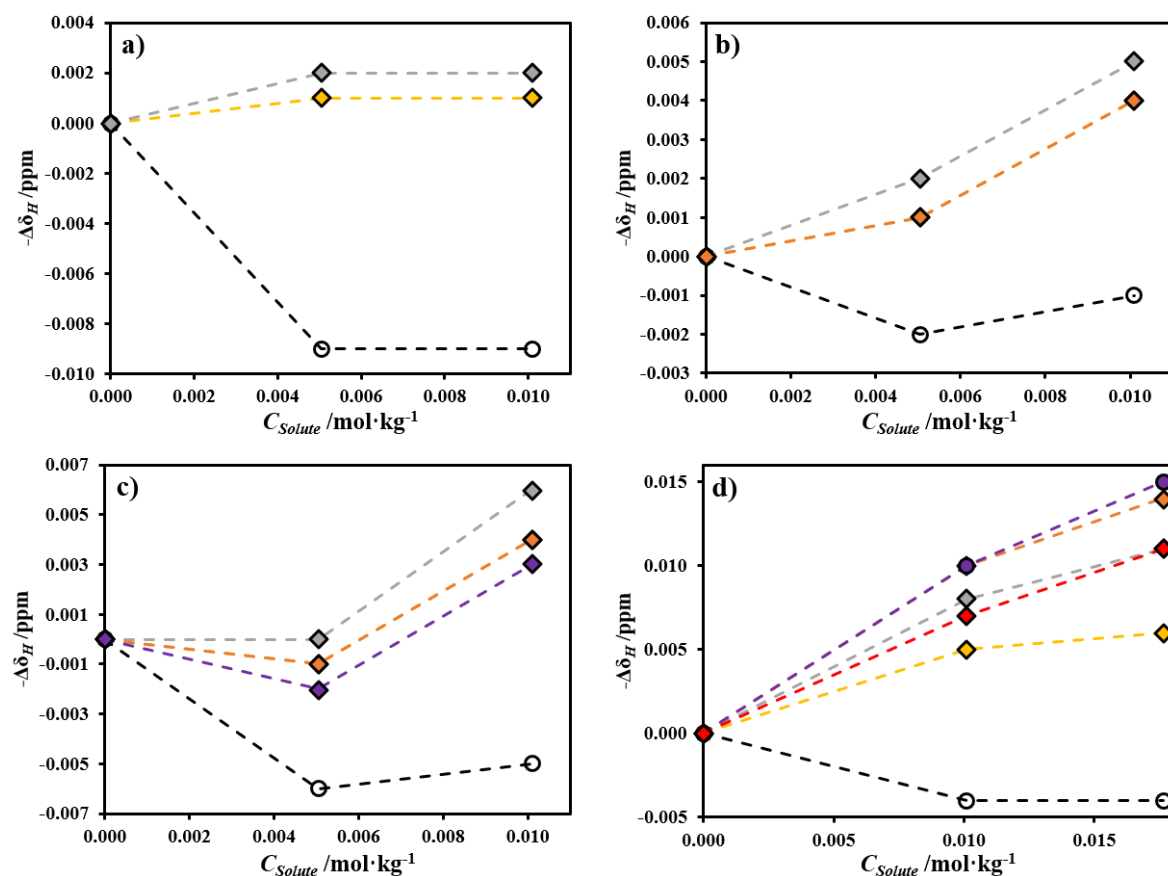


Figure S3. Change in chemical shift of the protons ($-\Delta\delta_H$) associated to water and several methyl groups of a) [1.0.0], b) [2.0.0], c) [3.0.0] and d) [5.0.0] dissolved in water (0.4 mol/kg) as a function of syringic acid concentration. Similar data for [4.0.0] is reported in the main text (Figure 1). Legend: -○- water; -◇- 2nd carbon; -◇- 4th carbon; -◇- 5th carbon; -◇- 6th carbon; -◇- 7th carbon; -◇- 8th carbon. For [5.0.0] the peaks from the hydrogens of the 6th and 7th carbon are undistinguishable and are represented as -●-.

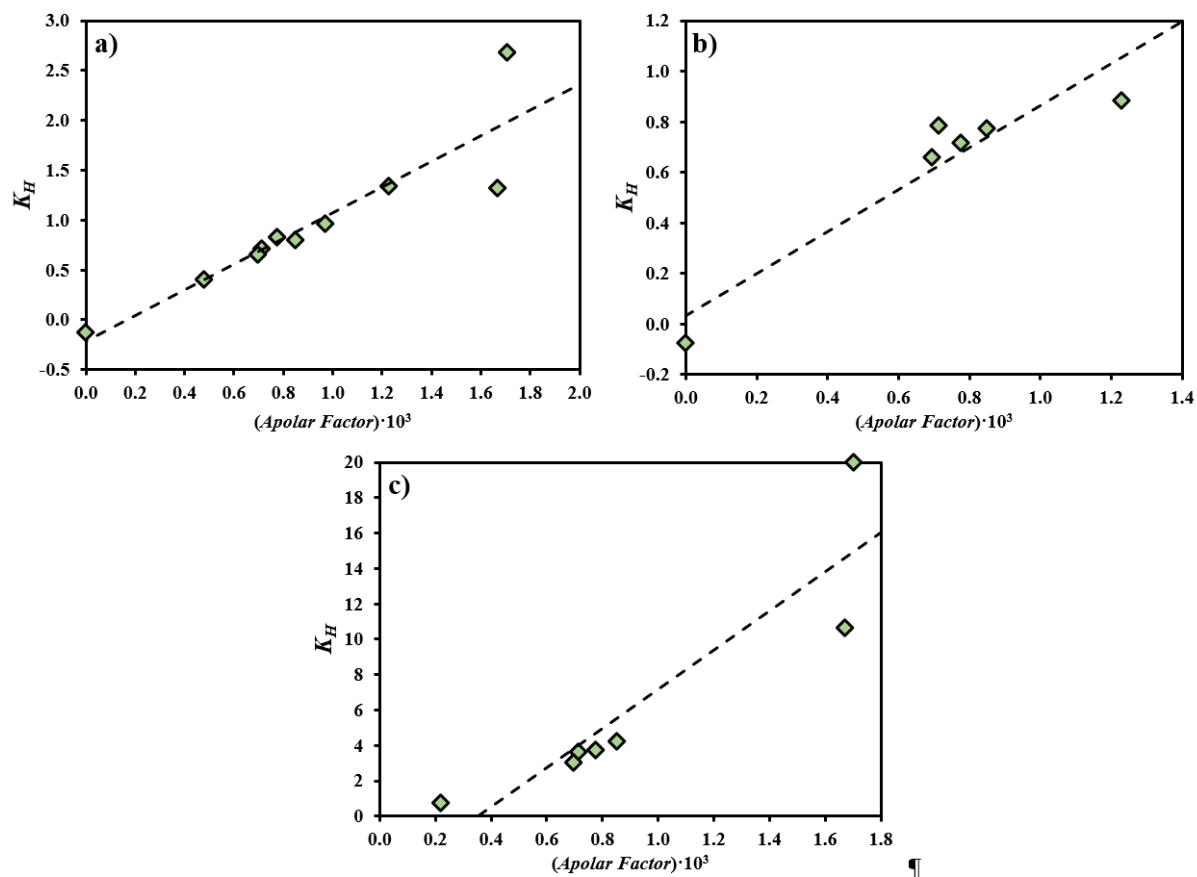


Figure S4. Setschenow constants of a) vanillin,⁵ b) gallic acid⁵ and c) ibuprofen⁶ for chloride-based ionic liquid hydrotropic systems as a function of the apolar factor of the ionic liquid. The dashed lines are the straight lines fitted to the data using the least squares method.

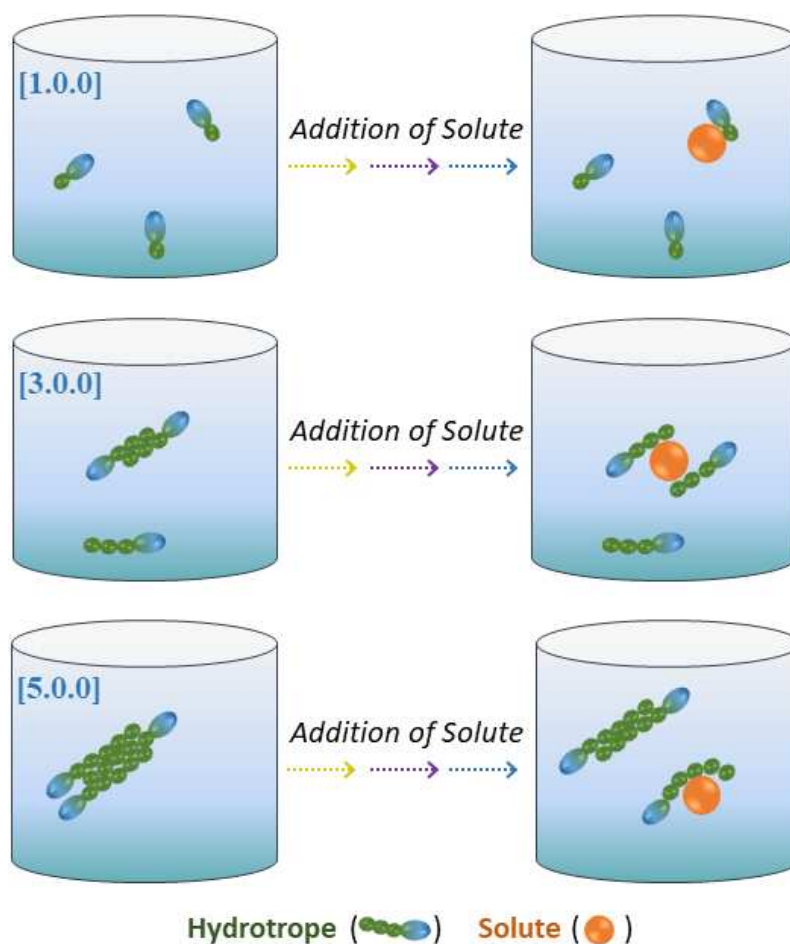


Figure S5. Schematic illustration of the hydrotrophy mechanism, evidencing the main findings in this work. In the first case, apolarity of the hydrotrope is small and the driving force for aggregation is low; in the second case, apolarity of the hydrotrope is equal to that of the solute and the driving force for aggregation is maximized, resulting in more hydrotrope molecules aggregated around the solute; in the third case, apolarity of the hydrotrope is greater than that of the solute and, thus, driving force for hydrotrope-hydrotrope aggregation is larger than that of hydrotrope-solute aggregation.

References

- 1 B. P. Soares, D. O. Abranches, T. E. Sintra, A. Leal-Duaso, J. I. García, E. Pires, S. Shimizu, S. P. Pinho and J. A. P. Coutinho, *ACS Sustain. Chem. Eng.*, 2020, **8**, 5742–5749.
- 2 TURBOMOLE V7.1 2016, a development of University of Karlsruhe and Forschungszentrum Karlsruhe GmbH, 1989-2007, TURBOMOLE GmbH, since 2007; available from <http://www.turbomole.com>.
- 3 COSMOtherm, Release 19; COSMOlogic GmbH & Co. KG, <http://www.cosmologic.de>.
- 4 F. Eckert and A. Klamt, *AIChE J.*, 2002, **48**, 369–385.
- 5 A. F. M. Cláudio, M. C. Neves, K. Shimizu, J. N. Canongia Lopes, M. G. Freire and J. A. P. Coutinho, *Green Chem.*, 2015, **17**, 3948–3963.
- 6 T. E. Sintra, K. Shimizu, S. P. M. Ventura, S. Shimizu, J. N. Canongia Lopes and J. A. P. Coutinho, *Phys. Chem. Chem. Phys.*, 2018, **20**, 2094–2103.